PROTEINS
STRUCTURE ■ FUNCTION ■ BIOINFORMATICS

Polyglutamine fibrils are formed using a simple designed β-hairpin model

Melanie H. Smith, Timothy F. Miles, Molly Sheehan, Katherine N. Alfieri, Bashkim Kokona, and Robert Fairman*

Department of Biology, Haverford College, Haverford, Pennsylvania 19041

ABSTRACT

Polyglutamine repeats are found in proteins associated with many neurodegenerative diseases. These repeats are responsible for intracellular protein aggregation that resemble amyloid plaques and contain the hallmarks of cross-β fibrillar structures. Recent work has suggested that the glutamines are involved in aggregation through two possible mechanisms: one involving only side-chain hydrogen bonding and a second involving interdigitation of the glutamines with tight van der Waal's packing (steric zipper model). We are interested in determining which interactions are particularly involved in early assembly processes and have developed a β-hairpin model system to address this problem. Our model system is designed to stabilize a putative high-energy nucleating structure to provide a window to view early assembly processes. We have applied spectroscopy tools (circular dichroism, infrared, and dynamic light scattering) to probe the self-assembly of β-sheet fibrils. These experiments established the conditions to study fibrillar morphology using atomic force microscopy. We show that fibrils are short with minimal lateral growth, suggesting that this may be a good model system for studying early assembly steps.

Proteins 2010; 78:1971–1979.

Key words: β-hairpin; β-sheet; polyglutamine fibrils; circular dichroism spectropolarimetry; Fourier transform infrared spectroscopy; atomic force microscopy; dynamic light scattering.

INTRODUCTION

Amyloid fibrils are insoluble, well-structured aggregates of misfolded protein that have been implicated in a number of prevalent, and largely neurodegenerative, human diseases.[1] Although they can be formed by a variety of natural proteins and synthetic peptides, all amyloid has a common cross-β structure.[2] In this structure, β-sheets are elongated in the direction of backbone hydrogen bonding or perpendicular to the strand direction (referred to as lateral assembly). The sheets can themselves assemble facially to form multiple layers. Side-chain interactions with other side chains or with the backbone can influence the kinetics and stability of amyloid formation.[3] Hydrogen bonding,[4,5] aromatic stacking,[4,6] and hydrophobic interactions[7,8] have all been implicated in these interactions, thus amino acid composition can play a role in self-assembly. One well-known sequence pattern that is associated with disease includes the polyglutamine repeat. There are at least nine genetically distinct polyglutamine diseases, most notably among which is Huntington's disease.[9] Within these diseases, the length of the polyglutamine repeat, determined by the size of a CAG trinucleotide repeat expansion in the gene for the disease-causing protein, often influences disease severity.[10] In addition, the frequency of amyloid-like inclusions tends to increase with the length of the repeat sequence.[11]

There are currently multiple models for the precise nature of the glutamine interactions that govern the formation and stability of amyloid fibrils. Based on modeling and electron diffraction data for $D_2Q_{15}K_2$, it has been proposed that the glutamine side chains form intrasheet hydrogen bonds to create "polar zipper" structures, in which the glutamine interactions principally involve H-bonding interactions between their amide groups.[5] More recently, in a review of this earlier work, it was proposed instead that a minor rearrangement of the glutamine side-chain geometries would more fully satisfy their hydrogen bonding potential.[12] Furthermore, this reorientation of intrasheet glutamine hydrogen bonding creates side-chain ridges that are self-complementary and interlock upon facial assembly, resulting in close

Additional Supporting Information may be found in the online version of this article.

Abbreviations: AFM, atomic force microscopy; ATR-FTIR, attenuated total reflectance Fourier transform infrared spectroscopy; CD, circular dichroism spectropolarimetry; DLS, dynamic light scattering; FMOC, fluorenyl methoxycarbonyl; MALDI-TOF, matrix-assisted laser desorption ionization time-of-flight spectrometry; RP-HPLC, reversed-phase high-performance liquid chromatography; TFA, trifluoroacetic acid.

Grant sponsor: NSF; Grant number: MCB-0516025; Grant sponsors: Arnold and Mabel Beckman Foundation, Haverford College (HHMI Undergraduate Science Education Program).
*Correspondence to: Robert Fairman, Department of Biology, Haverford College, 370 Lancaster Ave, Haverford, PA 19041. E-mail: rfairman@haverford.edu
Received 17 November 2009; Revised 16 February 2010; Accepted 19 February 2010
Published online 9 March 2010 in Wiley InterScience (www.interscience.wiley.com).
DOI: 10.1002/prot.22713

van der Waal's contacts between the glutamine methylene groups and has been referred to as a "steric zipper" interaction.[12] Both assembly paradigms have been observed for the same sequence based on the crystal structure of GNNQQNY[13] in which β-sheets associate via two different interfaces. β-Sheets are either involved in a "dry" interface, similar to that proposed earlier,[12] characterized by the formation of a steric zipper of interlocking side-chain ridges that exclude all but two water molecules or a "wet" interface in which the sheets are hydrated so that side chains on adjacent sheets form water-bridged hydrogen bonds. Multiple steric zipper isoforms, which differ in the orientation of the interacting β-sheets, have been identified in the crystal structures of various fibril-forming proteins, suggesting that the dry interface may be a common and preferred atomic arrangement in mature fibrils.[14,15] A growing body of evidence, however, suggests that the soluble intermediates and not the mature fibrils are the cytotoxic species responsible for the pathogenesis of amyloidoses.[16,17] Thus, understanding the interactions that govern the initial lateral and facial associations, and consequent stabilization of smaller intermediates, is of particular import.

Others have introduced a model that emphasizes the importance of β-sheet stability over facial lamination suggesting that fibers initially form through β-hairpin intermediates.[18] An elegant study, in which a sequence rich in polyglutamines is punctuated with prolines, supports a model of hairpin formation as an important intermediate in polyglutamine aggregation.[19] In these structures, hydrogen bonding is likely to be highly dynamic[18,20] with the folding and stability of the structure primarily due to cross-strand hydrophobic interactions and turn formation.[21,22] Initial assembly is thus believed to be driven largely by hydrophobic interactions in which a hydrophobic cluster forms allowing a greater proportion of the hairpin to acquire a β-sheet conformation.[21,23] Initial β-sheets may be highly dynamic, with individual units undergoing repeated detachment and annealing before arriving at this hydrophobic cluster configuration capable of supporting further aggregation.[24] Even in mature fibrils where β-strands buried within the core of the fibril are not solvent accessible, strands on the edges undergo repeated dissociation and reassociation.[25] Given this knowledge, initial associations of polyglutamine-containing β-strands may be driven by hydrophobic interactions involving close contacts between their methylene groups, akin to the polyglutamine steric zipper model. The stable formation of hydrogen bonds between glutamine side chains is thought to correlate with the assembly of the peptide into higher order, β-sheet structures and eventually amyloid-like fibrils. However, the role of glutamine interactions proposed by these models in fibril formation and stability has not been experimentally shown in solution.

Biomaterials groups have also shown an interest in the ability of peptides to self-assemble into fibrils for the construction of hydrogels and have sought to optimize and control the formation of these structures through the modulation of intra- and interpeptide interactions to promote folding and association, respectively.[8,26] For example, a peptide model system has been developed in which a pH switch was used to relieve electrostatic repulsive interactions between lysine residues and thus could be used as a triggering mechanism for the hydrophobically driven folding of a β-hairpin structure.[8] This then would facilitate both lateral and facial assembly of the peptide into a fibrillar hydrogel. A new glutamine-rich peptide system based on this β-hairpin model was thus designed to investigate the role of glutamine side chains in the assembly of amyloid-like fibrillar intermediates, and its sequence is described below.

METHODS

Modeling of a β-hairpin structure and dihedral angle determination was carried out through energy minimizations using INSIGHT II 2000.1 (Biosym Technologies, San Diego, CA) in DISCOVER by using a combination of steepest descents and conjugate gradients with a cvff force field to optimize the structure. All potentials, partial charges, and formal charges were taken into account. Modeling of higher order structures was carried out using Discovery Studio (Accelrys, San Diego, CA). Glutamine side-chain Cα-Cβ-Cγ torsion angles were adjusted to values described by Sikorski and Atkins to optimize H-bonding and to avoid steric overlap upon interdigitation of the glutamines as described in their steric zipper model.[12] Automated bump checks were applied in the process of docking two hairpins in creating the steric zipper model. Parallel and antiparallel conformations of the two hairpins appear equally plausible in this modeling exercise.

The disulfide crosslinked form of the tCQ8 peptide (acetylated at the N-terminus and amidated at the C-terminus) was purchased in crude form from AnaSpec (Fremont, CA). The peptide was purified by RP-HPLC using a mobile phase of water and acetonitrile (both containing 0.1% TFA) on a Varian ProStar system (Walnut Creek, CA) equipped with a Varian Dynamax semipreparative C18 column. The peptide was subsequently lyophilized and kept in a dessicator at −20°C for long-term storage. The identity of the product was verified by MALDI-TOF mass spectrometry, with the experimental molecular mass of 2724.1 Da in agreement with the theoretical molecular mass of 2724.3 Da. Quantitative conversion to the disulfide crosslinked form was confirmed using the Ellman's assay.[27] Concentrations of the peptide solutions were determined by a modified ninhydrin procedure.[28,29]

CD data were collected on an Aviv Biomedical Model 202-01 or Model 401-01 circular dichroism spectropolarimeter (Lakewood, NJ). Wavelength scans were performed in the range 180–260 nm at room temperature

using either a 0.2-mm path length cylindrical cell or a 1-mm rectangular cell, depending on peptide concentration. A step size of 0.5 nm with 3 s of averaging time was used. All measurements were taken using a bandwidth of 1.5 nm. Spectra were offset to zero at a reference point of 260 nm and blank subtracted.

ATR-FTIR spectra were collected using a Vertex 70 instrument (Bruker Optics, The Woodlands, TX) equipped with Opus version 5.5 software. Samples dissolved in water were dried onto CaF_2 windows and monitored at room temperature in the range of 1000–4000 cm^{-1}, using a resolution of 1 cm^{-1} and a total of 128 scans. Samples prepared on mica for atomic force microscopy (AFM) imaging were also measured using a single reflection GATR accessory (Harrick Scientific Products, Pleasantville, NY) designed for analyzing thin coatings on surfaces to determine the secondary structure of the peptide deposited on this surface. The GATR-FTIR samples were scanned at room temperature in the range of 850–4000 cm^{-1}, using a resolution of 2 cm^{-1} and a total of 512 scans. Second-order derivative analysis of FTIR spectra was performed using Origin, with smoothing using a second-order polynomial with averaging over a seven point window.

AFM data were collected in tapping mode by using a Bioscope AFM (Digital Instruments, Santa Barbara, CA) to obtain size and shape information for polymers deposited under various conditions. Cantilevers were obtained from Nanodevices Metrology Probes (Redding, CA). The tips were tested as needed against precisely engineered gold nanospheres and discarded if the measured sizes were significantly aberrant. Samples were incubated on a freshly cleaved mica surface for 10 min in a constant humidity chamber, rinsed with sterile water for ~30 s, and blown dry. Images prepared using a linear gray scale color table were transferred from the Nanoscope data for analysis using SigmaPro v. 5. Heights were analyzed by tracing along the filament axes, and ~80% of the filaments were measured in this way. Lengths were analyzed using only well-defined individual filaments, excluding any filaments with kinking or branching. Background intensity was corrected and normalized according to a procedure described previously.[30] Data were transferred to Origin for graphical presentation.

Dynamic light scattering (DLS) experiments were carried out using a DynaPro-MS/X molecular sizing instrument (Wyatt Technology, Santa Barbara, CA) equipped with an 825-nm laser and set at 10% power. Instrument operation, data collection, and analysis were managed using the Dynamics (V6) software interface. A 1 m*M* sample of tCQ8 in 12 m*M* sodium borate, pH 8.5, was analyzed at 20°C in a freshly cleaned cuvette to reduce dust contamination. A set of eight independent measurements (30 runs each) were made, and the time-dependent fluctuations in the scattered light were analyzed using a second-order correlation function. This correlation function was fitted to determine the number of decay rates, representing the different size distributions present in the sample. The decay rates were converted into apparent diffusion constants for calculation of the approximate hydrodynamic radii for each size distribution.

RESULTS AND DISCUSSION

A peptide, tCQ8, was designed to contain two stretches of alternating glutamine and lysine amino acids separated with a ^{D}Pro-^{L}Pro type II′ β-turn[31] and disulfide cross-linked by cysteines placed at the N- and C-termini (see Fig. 1). The prolines offer ideal geometries for this type of turn and hinder the free rotation of the backbone, thus reducing the entropic penalty of turn formation.[21] The use of prolines to stabilize hairpin structures in polyglutamine repeats has been reported previously.[19] In addition, the serine in the *i+3* position of the turn can further stabilize it through side chain–main chain hydrogen bonding.[26] We chose to cyclize our peptide using disulfide bonds as extensive experimentation with a non-cyclized variant showed it to be unable to adopt a significantly populated β-hairpin secondary structure. It has been shown that such cyclization further promotes the stability of a β-hairpin structure.[32,33] The placement of the lysines is based on work from the Schneider lab[8,26] so that the β-hairpin conformation would be unstable at near neutral pH conditions because of unfavorable electrostatic repulsive interactions but could acquire structure upon a pH jump to basic conditions, in which the lysines are at least partially deprotonated. Our goal in stabilizing the hairpin structure was to reduce the nucleation penalty in forming this early intermediate in the self-assembly process in the hopes that we could significantly populate early assembly intermediates (see Fig. 1).[34] Although the minimum number of glutamines per β-strand required for aggregation under reasonable peptide concentration conditions and experimentally accessible time regimes has been shown to be seven,[19] we decided to include only four glutamine residues per strand (eight total for the hairpin construct) in the hopes that the engineered turn and disulfide bond would act to sufficiently stabilize the monomeric hairpin structure. By alternating the glutamines with the lysines, the glutamines would project on one face of the hairpin structure to create the possibility of an amphipathic β-sheet fibril. Importantly, the electrostatic repulsive nature of the lysine faces should limit the extent of facial assembly to a bilayer with glutamines defining the interface, thus providing a method of control for the measurement of intersheet distances using AFM.

To show that tCQ8 is unfolded under conditions when the lysines are fully protonated, we initially measured the CD spectrum using 1.0 m*M* peptide in 0.01*M* HCl (pH

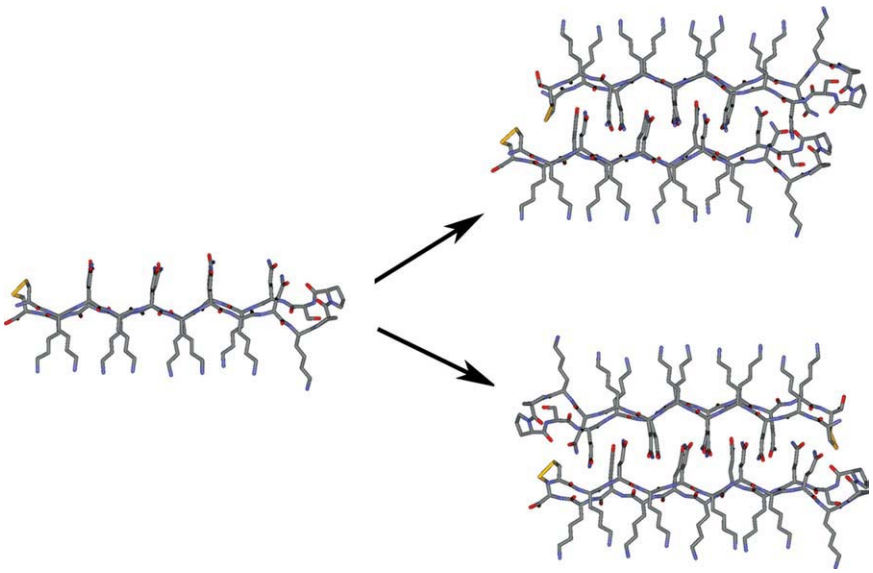

Figure 1

Steric zipper model of the tCQ8 β-hairpin. The peptide sequence modeled here is Ac-CKQKQKQKQK^{D}PPSQKQKQKQKC-CONH$_2$. tCQ8 is designed to form a β-hairpin composed of alternating glutamine and lysine residues in the two β-strands joined by a β-turn sequence containing ^{D}Pro-^{L}Pro at the *i, i+1* and *i, i+2* positions. The peptide is cyclized by disulfide bonds between cysteines placed at the N- and C-terminal positions. When protonated, the lysine residues repel each other promoting an unfolded state, thus pH and salt may be used to regulate the assumption of β-hairpin structure. Once in a hairpin conformation, the peptide may assemble laterally and facially to form extended fibrils with the glutamines at the interface. The figure shows models of facial assembly, involving steric zipper-type interactions, containing either parallel (top) or antiparallel (bottom) arrangements of the two hairpins with respect to one another.

2.0). The CD spectrum shows a slight minimum at 223 nm and a more intensive minimum at 204 nm, indicative of a largely unfolded peptide with β-turn characteristics (see Fig. 2).[35] As expected, the peptide is largely unfolded at pH 7.0 as well (Supplementary Information Fig. S1); residual structure at this pH may come from partial electrostatic screening owing to the buffer concentration. At pH 2.0, the peptide remains unfolded at high concentrations for long periods of time, thus providing a convenient condition for storing stock solutions. In contrast, a 1.0 m*M* sample of tCQ8 dissolved in 12 m*M* sodium borate, pH 8.5, in which the lysines are now significantly deprotonated, showed conversion to a β-sheet spectrum within seconds, as judged by CD, with a well-defined minimum at 218 nm. Peptides with similar lysine composition can show pK_a shifts in their ε-amino groups as low as 9.0, providing greater than 10% deprotonation at this higher pH.[36]

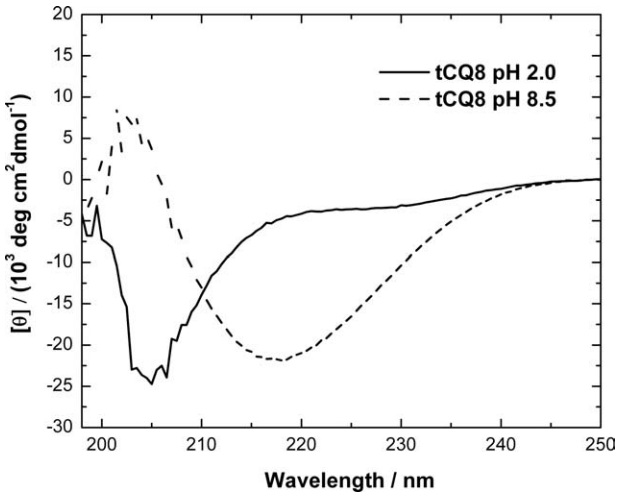

Figure 2

pH regulates the acquisition of structure in tCQ8. Spectra are measured using 1.0 m*M* tCQ8 dissolved either in 0.01*M* HCl or in 12 m*M* sodium borate, pH 8.5.

When the peptide is left to stand for at least a day, the peptide forms large aggregates as evidenced by first an increase in intensity of the 218-nm band and a subsequent red shifting of the band, followed by a decrease in intensity as the material begins to fall out of solution (Supplementary Information Fig. S2). Red shifting is an artifact of increased light scattering, which decreases the extinction nonlinearly with decreasing wavelength.[37–40] Interestingly, simply inverting the cuvette several times results in dissolution of the large aggregates while retaining all of the β-sheet characteristics, suggesting that the material is readily reversible. This can be seen by the complete recovery of the CD spectrum even after 6 days

of incubation (Supplementary Information Fig. S2). As a further test of reversibility of the large aggregates, the 1.0 m*M* samples were diluted 10-fold to 0.1 m*M*. Whether the sample was diluted immediately after preparation of the sample or after 7 days of incubation, large-scale aggregation was reversed while maintaining all the β-sheet characteristics [Fig. 3(b)]. Dilution or mechanical disruption therefore appears to reduce the peptide back to form either monomeric β-hairpins or, at most, small β-sheet fibrils.[34] This hypothesis was tested further through a combined FTIR and AFM approach, looking at materials that had been incubated for several days and testing the effects of dilution on the macromolecular structures formed.

In general, CD spectropolarimetry is not as reliable for the unequivocal assignment of β-sheet structures when compared with α-helical structures. Therefore, samples of tCQ8 shown to assume a β-sheet structure and aggregate, as evidenced by CD, were analyzed by the complementary method of ATR-FTIR.[41] A 1.0 m*M* tCQ8 sample was prepared in D_2O in 12 m*M* sodium borate, pH 8.5,

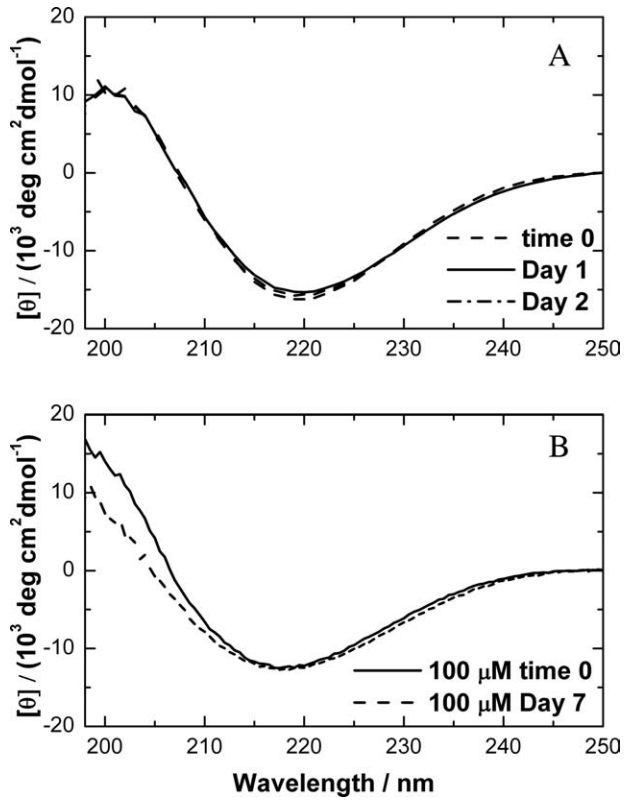

Figure 3

Assembly is rapid and resistant to dilution. tcQ8 was dissolved at 1.0 m*M* peptide concentration in 12 m*M* sodium borate, pH 8.5, and CD spectra were collected over time. (**a**) Spectra collected at 1.0 m*M* tCQ8. (**b**) After incubation at a concentration of 1.0 m*M* tCQ8 for the times stated, samples were removed and diluted to 100 μ*M* peptide concentration for CD data collection.

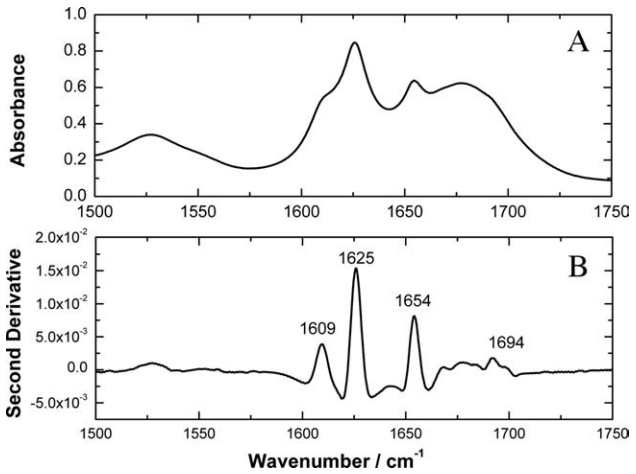

Figure 4

tCQ8 β-structure is also evident by FTIR. (**a**) ATR-FTIR spectrum of 1.0 m*M* tCQ8 dissolved in H_2O containing 12 m*M* sodium borate, pH 8.5, deposited onto a CaF_2 window and dried. (**b**) Second-derivative analysis of the data in (a) reveals major peaks at 1609, 1625, 1654, and 1694 cm^{-1}. The peak at 1625 cm^{-1} is consistent with that expected for β-sheet fibrils. A second, minor peak in the range of 1668–1687 cm^{-1} is expected for such structures but may be obscured by residual TFA in the samples from the peptide purification protocol. It is intriguing that a weak band is present at 1694 cm^{-1} although it lies somewhat outside the range expected for the aggregated β-sheet conformation. The peaks at 1609 and 1654 cm^{-1} likely arise from the amide groups from the glutamine side chains.

to measure the FTIR spectrum in solution for comparison to the CD experiment. Use of D_2O in place of H_2O minimizes the interfering H_2O band at around 1640 cm^{-1} and aids in interpreting the secondary structure of the peptide. Under these conditions, tCQ8 exhibited a strong characteristic band at 1619 cm^{-1}, supporting the conclusion from CD that the peptide forms β-sheet and further supports evidence of aggregation based on the degree of red shifting of this band from that expected for a canonical β-sheet spectrum (Supplementary Information Fig. S3). An interesting feature in this same spectrum is the presence of a band at 1609 cm^{-1}, most likely due to the NH_2 deformation frequency of the side-chain amide group[42]; the intensity of this band is consistent with a well-ordered arrangement of the side chains. Overall, the D_2O spectrum required careful second-derivative analysis to extract out reliable information; this prompted us to prepare samples in H_2O under the same conditions and then dry them directly onto CaF_2 windows to improve the signal to noise ratio and to provide higher quality spectra. The spectrum in Figure 4(a) confirms the evidence for aggregated β-sheet that was observed in D_2O, with a well-defined β-sheet band at 1625 cm^{-1}. This band is slightly shifted relative to the D_2O band; this solvent effect is consistent with what has been reported in the literature.[43] Although the ϵ-amino groups of lysines also may have a band around

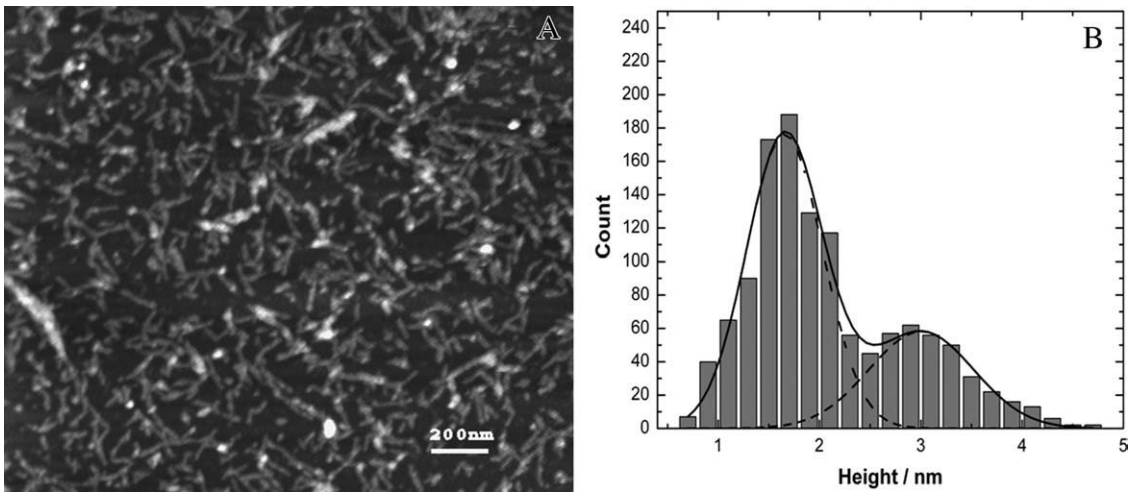

Figure 5

AFM analysis of tCQ8 fibrils. (**a**) AFM image was taken using 0.1 m*M* tCQ8 in 12 m*M* sodium borate, pH 8.5, after 7 days of incubation. The image was taken top-down at 1 Hz. (**b**) Before the height analysis, the image was flattened for tilt, streaks, and parabolic artifacts. Height measurements were then made and binned in 0.2-nm increments. The black curve shows a bimodal Gaussian distribution fit to the data with peaks centered at 3.0 ± 0.1 nm and 1.66 ± 0.03 nm.

1625 cm^{-1}, we ruled out this assignment as FTIR spectra of unfolded samples of a related hairpin peptide do not show this feature. The band at 1609 cm^{-1} is assigned to the side-chain amide NH_2 deformation as described above for the D_2O sample. An additional feature that is prominent in the spectrum is a band at 1654 cm^{-1}, which may be either the CO stretch of the side-chain amide group of the glutamines or, less likely, some random-coil contribution to the sample. This latter conclusion is inconsistent with our interpretation of our CD spectra. Furthermore, model analysis of an acetylated and amidated tripeptide (sequence: KQK) supports the assignment of this band to the side-chain CO stretch (data not shown). The broader, featureless peak in the range 1670–1720 cm^{-1} is harder to interpret but may contain contributions from the β-turn, the amide I secondary band for an aggregated β-sheet (usually found in the range 1668–1687 cm^{-1}),[44] and residual TFA (typically seen at 1672 cm^{-1}).

Analysis of the morphology of the tCQ8 aggregates was probed by AFM. Samples of 1.0 and 0.1 m*M* tCQ8 were prepared and incubated for several days before deposition, drying, and imaging. Visualization of the morphology for the 1.0 m*M* peptide sample revealed a highly dense network of material involving a heterogeneous mixture of small fibrillar structures (Supplementary Information Fig. S4). Given the amount of material present, it was difficult to quantify the lengths and heights of these structures. Dilution of the peptide to 0.1 m*M* resulted in lower density of deposition on the mica surface, making it easier to discern individual fibrils [Fig. 5(a)]. Surface effects might exert sufficient force to change the noncovalent secondary structure of deposited protein-based materials. To test for this, the same sample that was imaged by AFM was then measured using ATR-FTIR using a single reflection horizontal accessory designed for analysis of thin films and coatings on opaque surfaces. For both the 1.0 and 0.1 m*M* tCQ8 samples, the spectra were identical to that observed for the solution experiments described above (see Fig. 6). Most

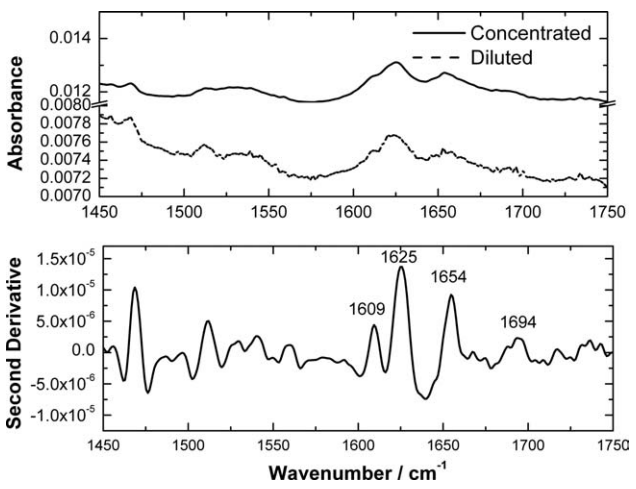

Figure 6

GATR-FTIR analysis of AFM sample. The sample prepared for AFM was measured directly using GATR-FTIR. Spectra data were collected at room temperature and averaged over 512 scans in the range 800–4000 cm^{-1}, using a resolution of 2 cm^{-1}.

notably, a peak at 1625 cm^{-1} is observed, with a weaker peak at 1694 cm^{-1}, identical to that shown in Figure 4, indicative of the presence of aggregated β-sheet.

Although widths of the fibrils might provide insight as to the orientation of the presumed β-sheet fibrils on the surface, because of well-known tip convolution effects, this cannot be accurately determined given the small size of the widths.[30,45] Instead, the most accurate measurements that can be made by this technique are the height(s) and lengths of the deposited material. Heights were measured by tracing as many of the fibrils as possible (>80% of the features) in SigmaPro and the resulting heights were binned and are presented in histogram form in Figure 5(b). There are two clearly defined populations of fibrils with the predominant material having a height of 1.66 ± 0.03 nm and a second minor component that has an average height of 3.0 ± 0.1 nm. An earlier study, looking at the fibrillar structure of residues 10–39 of the glutamine-rich yeast prion protein, Ure2p, also identified a height of about 1.6 nm by AFM.[46] The 1.66-nm height can be readily assigned to a single structural feature of cross-β fibrils. The features of such fibrils relevant to the AFM measurements include the length of the hairpin structure itself, which defines the width of a β-sheet (3.7 nm based on the lengths of the strands) and the height of the hairpins (1.0 nm, which is calculated to include the average projection of the side chains off either side of the hairpin plane as described below). Thus, the AFM-measured height most likely reflects the height of an integral number of β-sheets lying flat on the surface as the 3.7-nm value is too large relative to the measured value. With this reasonable assumption, the height can be interpreted in terms of the degree of lamination of the β-sheets, with the expectation that a β-sheet bilayer should dominate, based on previous work using such a lysine-rich hairpin model system. As the value of a β-sheet monolayer (1.0 nm) is significantly below that of the measured height of 1.66 nm, this suggests that the fibril must be forming a bilayer, consistent with that observed by the Schneider laboratory.[26,47]

Although more speculative, it is worth analyzing whether the measured height can distinguish between a bilayer in which the glutamines are interdigitated (steric zipper model) from one in which the bilayer interface is dominated by H-bonding between extended glutamines. Using crystal structures as a starting point for modeling the bilayer with a glutamine interface,[5,12,13,48] we found that the expected heights would be 2.0 nm for the steric zipper structure and 2.8 nm for the more expanded structure. The height of 2.0 nm is consistent with that reported in the Schneider work, from which our model system is derived.[49] Thus, the AFM-measured height of 1.66 nm is more consistent with that expected for the model involving interdigitation of the glutamines.[12] It is well established that experimentally determined heights using the AFM are typically 30% below calculated values, particularly for protein fibrils of the dimensions reported here, because of the elastic nature of peptide structures in response to the tapping of the AFM cantilever.[30,50,51] Thus, applying this correction factor, the height would be 2.20 nm or directly within the range for a steric zipper but significantly smaller than that expected for the more expanded structure.

The second, minor population of heights centered about 3.0 nm is much more difficult to interpret. It could be due to a greater degree of lamination of individual structures, overlap of bilayers due to greater density of deposition, or a twisting of the fibrils on the surface as has been observed for a variant of our model system previously.[47] We are continuing to investigate this morphological feature of our system.

Lengths were measured using the image in Figure 4 by tracing fibrils in a manner similar to that used for the height analysis. Given the complexity of the fibrils, kinked and branched structures were excluded and only clearly isolated fibrils were analyzed. The resulting measurements were binned, and a normal distribution was found, with an average length of 10.04 ± 0.70 nm as determined from a fit to a Gaussian function. Assuming a hairpin width of 0.5 nm (measured between pairs of C_a atoms across the hairpin structure), the 10-nm fibril lengths would contain ~20 hairpin units per β-sheet. We postulate that these units may be building blocks for the longer sized fibrils and could explain the punctate nature of the longer fibrils that are seen in some images. This size range is consistent with that seen by others.[52] The lengths are likely largely determined by the glutamine interactions as the hairpin model system used by the Schneider lab,[8,26] containing valines in place of the glutamines, forms much longer fibrils with distinctly different morphology.

It is possible that the preparation of the samples for AFM may skew the representation of the solution distribution. To measure fibril lengths in solution, we used DLS. DLS data of tCQ8 in 12 m*M* sodium borate, pH 8.5, show two distributions (Supplementary Information Fig. S5). The smaller distribution is well defined with moderate heterogeneity, containing fibrils with an average diameter of 16.7 ± 1.8 nm, in reasonable agreement with the AFM results. The second distribution is highly diffuse and asymmetric, with diameters ranging from 80 to 1100 nm. Some evidence for larger scale fibrils is evident in our AFM work particularly in the sample deposition at higher peptide concentrations (Supplementary Information Fig. S4).

We have shown, through spectroscopic characterization, that our model system can form aggregated β-sheet structures rapidly, making it amenable for further study of the kinetics and stability of polyglutamine sequences. Furthermore, AFM analysis of the morphology of the aggregated structures reveals that the lengths are consistent with that seen for other polyglutamine systems. The

lengths fall in the range expected for fibrillar intermediates, making this model system a good candidate for assessing important chemical characteristics, such as the role of the glutamine amide groups in regulating self-assembly. We show that these intermediate structures are dominated by bilayers in which the glutamines are intercalated, consistent with other work providing compelling evidence for tight intercalation of H-bonded glutamines, and referred to as steric zipper structures.

ACKNOWLEDGMENTS

The authors thank Dr. Feng Gai and Smita Mukherjee for the use of their ATR-FTIR instrument and help with data acquisition and Dr. William DeGrado for the use of his mass spectrometer and modeling software. They also thank Justin Meyerowitz, Andrew McNeal, and Kelsey Capron for excellent technical assistance, Dr. Casey Londergan for advice on FTIR experiments, and Dr. Joel Schneider for helpful advice on the β-hairpin system.

REFERENCES

1. Chiti F, Dobson CM. Protein misfolding, functional amyloid, and human disease. Annu Rev Biochem 2006;75:333–366.
2. Dobson CM. Protein folding and misfolding. Nature 2003;426:884–890.
3. Hughes RM, Waters ML. Model systems for beta-hairpins and beta-sheets. Curr Opin Struct Biol 2006;16:514–524.
4. Makin OS, Atkins E, Sikorski P, Johansson J, Serpell LC. Molecular basis for amyloid fibril formation and stability. Proc Natl Acad Sci USA 2005;102:315–320.
5. Perutz MF, Johnson T, Suzuki M, Finch JT. Glutamine repeats as polar zippers: their possible role in inherited neurodegenerative diseases. Proc Natl Acad Sci USA 1994;91:5355–5358.
6. Mahalakshmi R, Raghothama S, Balaram P. NMR analysis of aromatic interactions in designed peptide beta-hairpins. J Am Chem Soc 2006;128:1125–1138.
7. Calamai M, Taddei N, Stefani M, Ramponi G, Chiti F. Relative influence of hydrophobicity and net charge in the aggregation of two homologous proteins. Biochemistry 2003;42:15078–15083.
8. Schneider JP, Pochan DJ, Ozbas B, Rajagopal K, Pakstis L, Kretsinger J. Responsive hydrogels from the intramolecular folding and self-assembly of a designed peptide. J Am Chem Soc 2002;124:15030–15037.
9. Gatchel JR, Zoghbi HY. Diseases of unstable repeat expansion: mechanisms and common principles. Nat Rev Genet 2005;6:743–755.
10. Mitas M. Trinucleotide repeats associated with human disease. Nucleic Acids Res 1997;25:2245–2254.
11. Perutz MF. Glutamine repeats and neurodegenerative diseases: molecular aspects. Trends Biochem Sci 1999;24:58–63.
12. Sikorski P, Atkins E. New model for crystalline polyglutamine assemblies and their connection with amyloid fibrils. Biomacromolecules 2005;6:425–432.
13. Nelson R, Sawaya MR, Balbirnie M, Madsen A, Riekel C, Grothe R, Eisenberg D. Structure of the cross-beta spine of amyloid-like fibrils. Nature 2005;435:773–778.
14. Sawaya MR, Sambashivan S, Nelson R, Ivanova MI, Sievers SA, Apostol MI, Thompson MJ, Balbirnie M, Wiltzius JJ, McFarlane HT, Madsen A, Riekel C, Eisenberg D. Atomic structures of amyloid cross-beta spines reveal varied steric zippers. Nature 2007;447:453–457.
15. van der Wel PCA, Lewandowski JR, Griffin RG. Solid-state NMR study of amyloid nanocrystals and fibrils formed by the peptide GNNQQNY from yeast prion protein Sup35p. J Am Chem Soc 2007;129:5117–5130.
16. Stefani M, Dobson CM. Protein aggregation and aggregate toxicity: new insights into protein folding, misfolding diseases and biological evolution. J Mol Med 2003;81:678–699.
17. Poirier MA, Li HL, Macosko J, Cai SW, Amzel M, Ross CA. Huntingtin spheroids and protofibrils as precursors in polyglutamine fibrilization. J Biol Chem 2002;277:41032–41037.
18. Ciani B, Jourdan M, Searle MS. Stabilization of beta-hairpin peptides by salt bridges: role of preorganization in the energetic contribution of weak interactions. J Am Chem Soc 2003;125:9038–9047.
19. Thakur AK, Wetzel R. Mutational analysis of the structural organization of polyglutamine aggregates. Proc Natl Acad Sci USA 2002; 99:17014–17019.
20. Colley CS, Griffiths-Jones SR, George MW, Searle MS. Do interstrand hydrogen bonds contribute to beta-hairpin peptide stability in solution? Chem Commun 2000:593–594.
21. Du D, Zhu Y, Huang CY, Gai F. Understanding the key factors that control the rate of beta-hairpin folding. Proc Natl Acad Sci USA 2004;101:15915–15920.
22. Muñoz V, Thompson PA, Hofrichter J, Eaton WA. Folding dynamics and mechanism of beta-hairpin formation. Nature 1997;390: 196–199.
23. Espinosa JF, MuÒoz V, Gellman SH. Interplay between hydrophobic cluster and loop propensity in beta-hairpin formation. J Mol Biol 2001;306:397–402.
24. Petty SA, Decatur SM. Intersheet rearrangement of polypeptides during nucleation of {beta}-sheet aggregates. Proc Natl Acad Sci USA 2005;102:14272–14277.
25. Carulla N, Caddy GL, Hall DR, Zurdo J, GairÌ M, Feliz M, Giralt E, Robinson CV, Dobson CM. Molecular recycling within amyloid fibrils. Nature 2005;436:554–558.
26. Rajagopal K, Ozbas B, Pochan DJ, Schneider JP. Probing the importance of lateral hydrophobic association in self-assembling peptide hydrogelators. Eur Biophys J 2006;35:162–169.
27. Rao US, Scarborough GA. Chemical state of the cysteine residues in the Neurospora crassa plasma membrane H(+)-ATPase. J Biol Chem 1990;265:7227–7235.
28. Crestfield AM, Moore S, Stein WH. The preparation and enzymatic hydrolysis of reduced and S-carboxymethylated proteins. J Biol Chem 1963;238:622–627.
29. Rosen H. A modified ninhydrin colorimetric analysis for amino acids. Arch Biochem Biophys 1957;67:10–15.
30. Rigotti DJ, Kokona B, Horne T, Acton EK, Lederman CD, Johnson KA, Manning RS, Kane SA, Smith WF, Fairman R. Quantitative atomic force microscopy image analysis of unusual filaments formed by the *Acanthamoeba castellanii* myosin II rod domain. Anal Biochem 2005;346:189–200.
31. Bean JW, Kopple KD, Peishoff CE. Conformational-analysis of cyclic hexapeptides containing the D-Pro-L-Pro sequence to fix beta-turn positions. J Am Chem Soc 1992;114:5328–5334.
32. Stotz CE, Topp EM. Applications of model beta-hairpin peptides. J Pharm Sci 2004;93:2881–2894.
33. Russell SJ, Blandl T, Skelton NJ, Cochran AG. Stability of cyclic beta-hairpins: asymmetric contributions from side chains of a hydrogen-bonded cross-strand residue pair. J Am Chem Soc 2003; 125:388–395.
34. Kodali R, Wetzel R. Polymorphism in the intermediates and products of amyloid assembly. Curr Opin Struct Biol 2007;17:48–57.
35. Gibbs AC, Bjorndahl TC, Hodges RS, Wishart DS. Probing the structural determinants of type II' beta-turn formation in peptides and proteins. J Am Chem Soc 2002;124:1203–1213.
36. Root BC, Pellegrino LD, Crawford ED, Kokona B, Fairman R. Design of a heterotetrameric coiled coil. Protein Sci 2009;18:329–336.
37. Arutyunyan AM, Rafikova ER, Drachev VA, Dobrov EN. Appearance of "beta-like" circular dichroism spectra on protein aggregation that is not accompanied by transition to beta-structure. Biochemistry (Mosc) 2001;66:1378–1380.

38. Benjwal S, Verma S, Röhm KH, Gursky O. Monitoring protein aggregation during thermal unfolding in circular dichroism experiments. Protein Sci 2006;15:635–639.
39. Dunetz JR, Sandstrom C, Young ER, Baker P, Van Name SA, Cathopolous T, Fairman R, de Paula JC, Akerfeldt KS. Self-assembling porphyrin-modified peptides. Org Lett 2005;7:2559–2561.
40. Soldi G, Bemporad F, Torrassa S, Relini A, Ramazzotti M, Taddei N, Chiti F. Amyloid formation of a protein in the absence of initial unfolding and destabilization of the native state. Biophys J 2005;89:4234–4244.
41. Kong J, Yu S. Fourier transform infrared spectroscopic analysis of protein secondary structures. Acta Biochim Biophys Sin (Shanghai) 2007;39:549–559.
42. Rahmelow K, Hubner W, Ackermann T. Infrared absorbances of protein side chains. Anal Biochem 1998;257:1–11.
43. Dzwolak W, Loksztejn A, Smirnovas V. New insights into the self-assembly of insulin amyloid fibrils: an H-D exchange FT-IR study. Biochemistry 2006;45:8143–8151.
44. Goormaghtigh E, Cabiaux V, Ruysschaert JM. Determination of soluble and membrane protein structure by Fourier transform infrared spectroscopy. III. Secondary structures. Subcell Biochem 1994;23:405–450.
45. Murray MN, Hansma HG, Bezanilla M, Sano T, Ogletree DF, Kolbe W, Smith CL, Cantor CR, Spengler S, Hansma PK, Salmeron M. Atomic force microscopy of biochemically tagged DNA. Proc Natl Acad Sci USA 1993;90:3811–3814.
46. Chan JCC, Oyler NA, Yau WM, Tycko R. Parallel beta-sheets and polar zippers in amyloid fibrils formed by residues 10-39 of the yeast prion protein Ure2p. Biochemistry 2005;44:10669–10680.
47. Nagarkar RP, Hule RA, Pochan DJ, Schneider JP. De novo design of strand-swapped beta-hairpin hydrogels. J Am Chem Soc 2008;130:4466–4474.
48. Sharma D, Shinchuk LM, Inouye H, Wetzel R, Kirschner DA. Polyglutamine homopolymers having 8-45 residues form slablike beta-crystallite assemblies. Proteins 2005;61:398–411.
49. Ozbas B, Rajagopal K, Schneider JP, Pochan DJ. Semiflexible chain networks formed via self-assembly of beta-hairpin molecules. Phys Rev Lett 2004;93(26 Part 1):268106.
50. Jiao Y, Schäffer TE. Accurate height and volume measurements on soft samples with the atomic force microscope. Langmuir 2004;20:10038–10045.
51. Knoll A, Magerle R, Krausch G. Tapping mode atomic force microscopy on polymers: where is the true sample surface? Macromolecules 2001;34:4159–4165.
52. Dahlgren PR, Karymov MA, Bankston J, Holden T, Thumfort P, Ingram VM, Lyubchenko YL. Atomic force microscopy analysis of the Huntington protein nanofibril formation. Nanomedicine 2005;1:52–57.

Supplementary Figures.

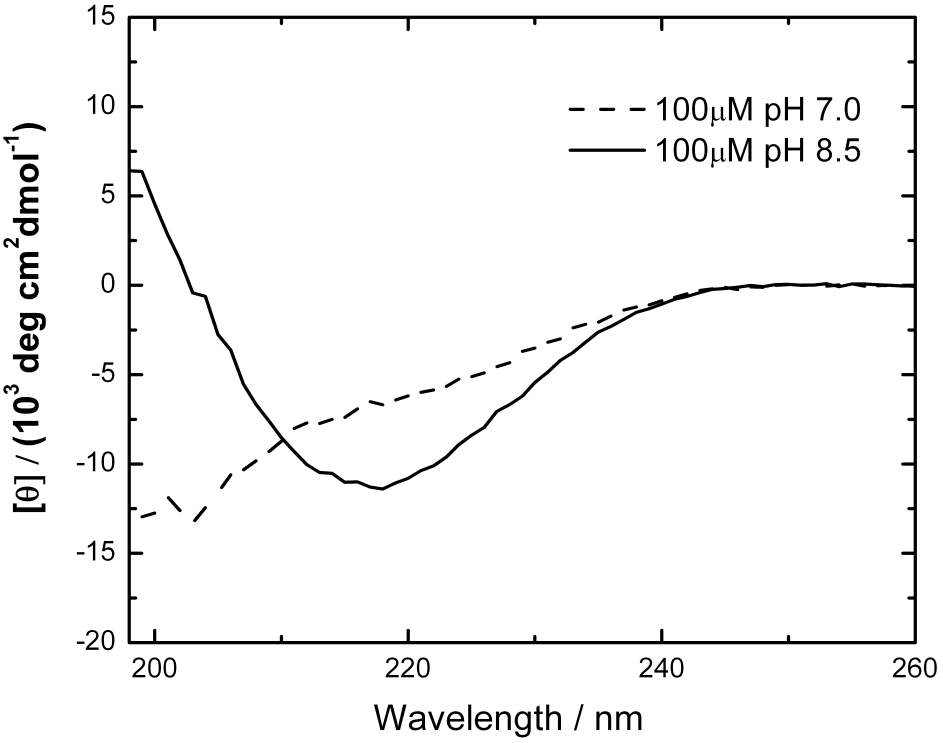

Figure S1. CD spectrum of 100 μM tCQ8 in 10 mM Tris-HCl, pH 7.0.

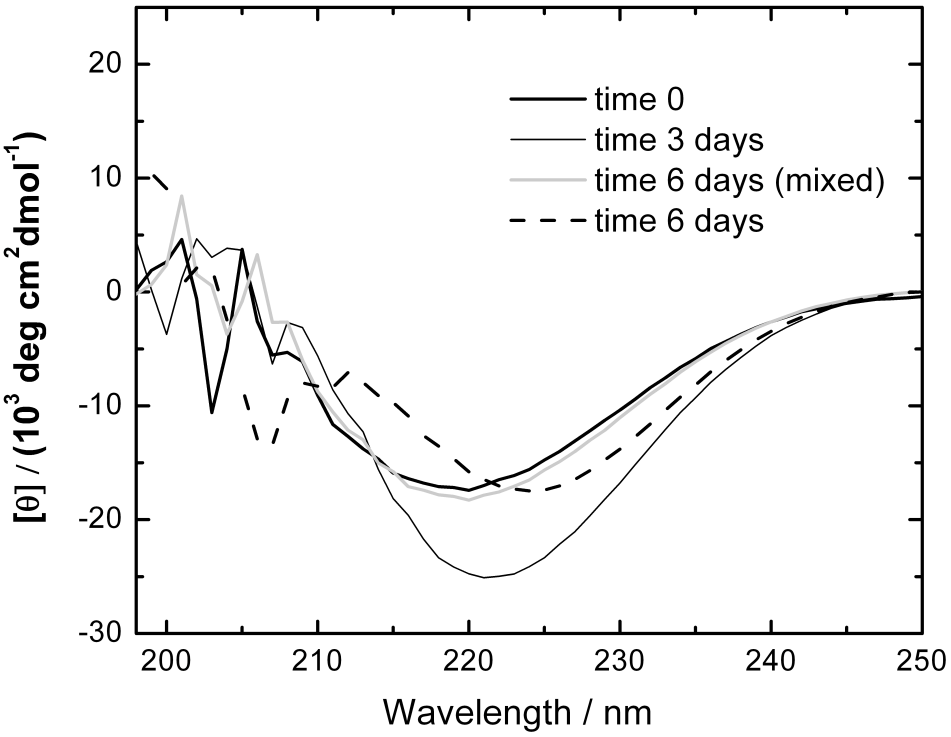

Figure S2. CD spectra as a function of time for 600 μM tCQ8 in 50 mM sodium borate, pH 8.5.

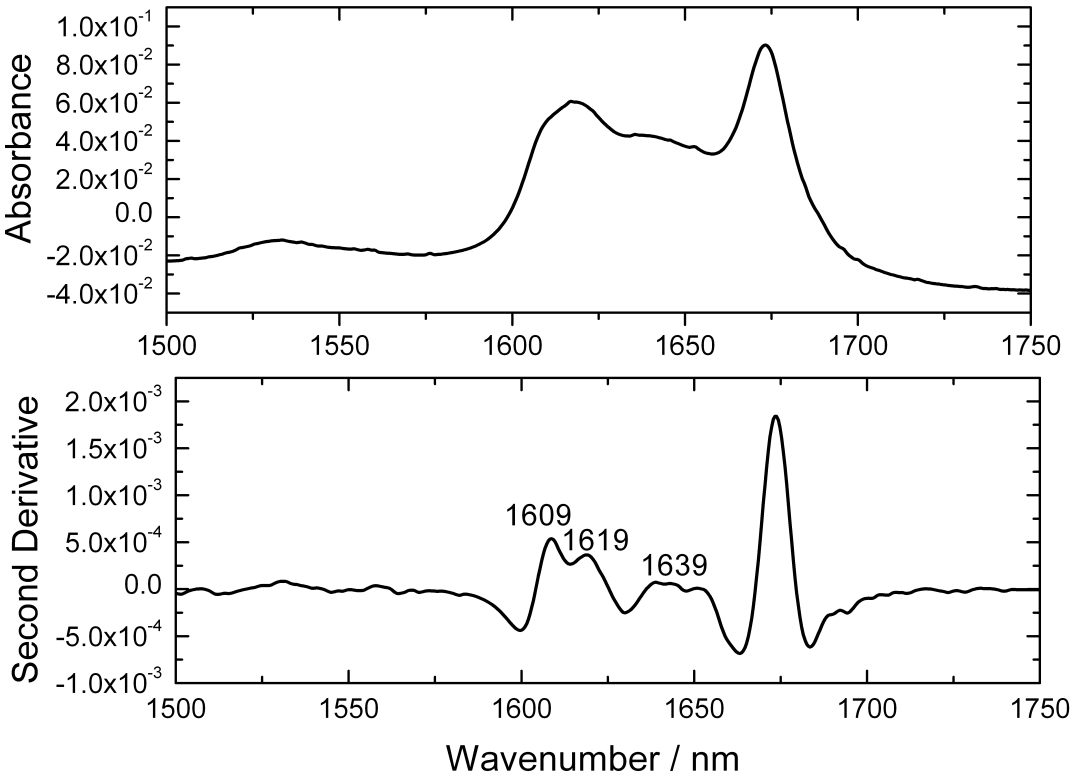

Figure S3. FTIR spectrum of 1 mM tCQ8 in 12 mM sodium borate, pD 9.0 in D_2O. Assignments of the bands are as follows: 1619 cm^{-1} represents the major CO stretch of the backbone for an aggregated β-sheet; 1609 cm^{-1} represents the deformation frequency of the unexchanged NH_2 group for the sidechain amides; 1639 cm^{-1} represents the CO stretch of the sidechain amide and is shifted relative to the 1654 cm^{-1} band seen for this same group in H_2O (Figure 4a). The peak at 1639 cm^{-1} and the unlabeled peak at around 1654 cm^{-1} suggest evidence for partial HD exchange in the backbone as well. The major peak at 1674 cm^{-1} represents residual TFA introduced during HPLC purification.

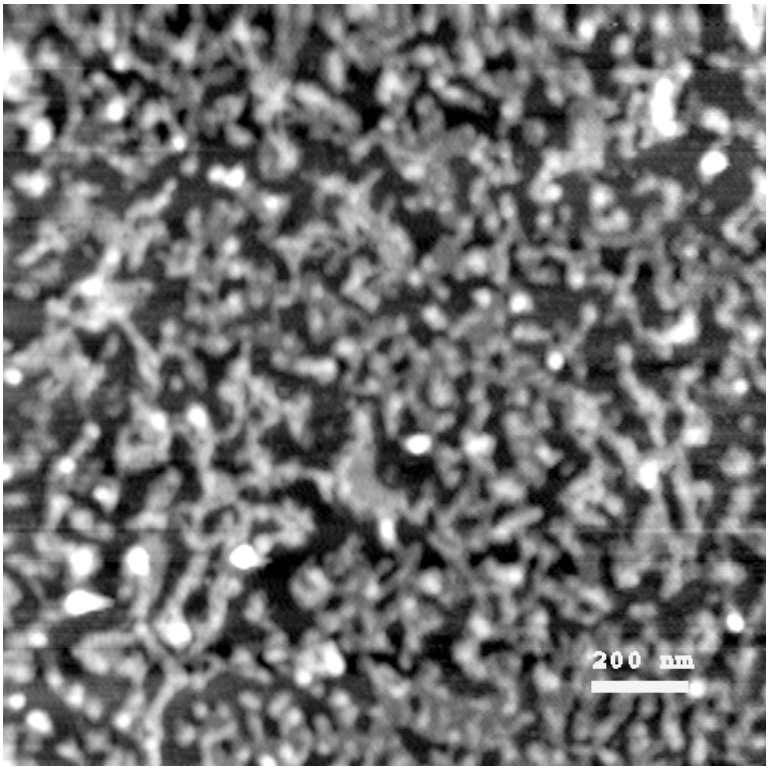

Figure S4. AFM image of tCQ8 fibrils from a sample containing 1 mM tCQ8 in 12 mM sodium borate, pH 8.5. Sample preparation is done under the same conditions as that reported in Figure 5.

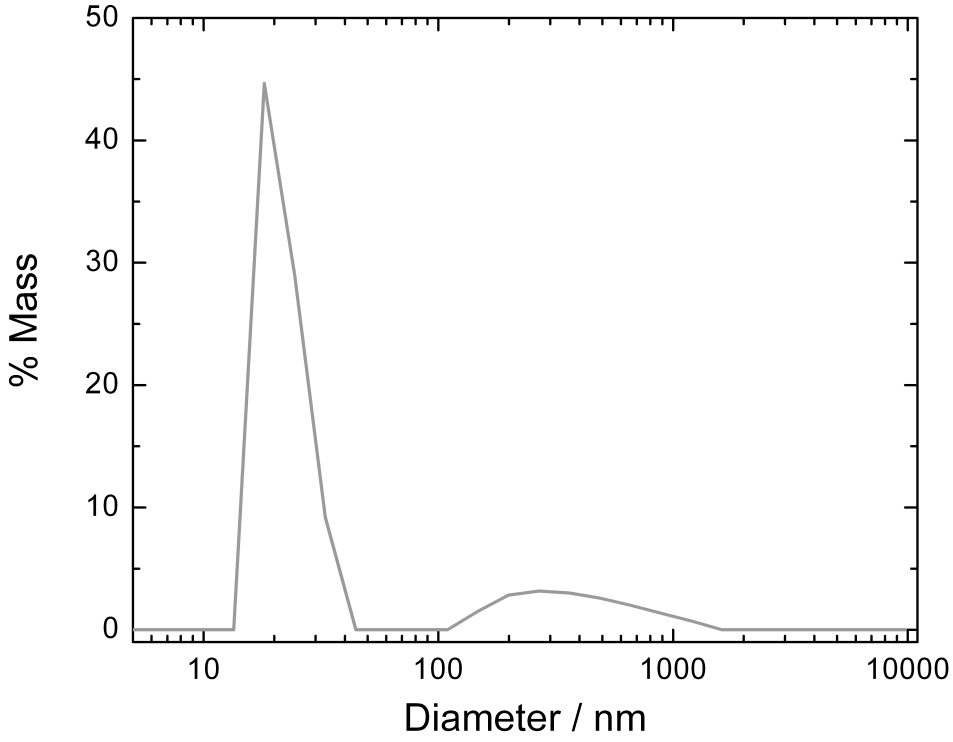

Figure S5. Mass distribution from a dynamic light scattering measurement of a 1mM tCQ8 sample prepared in 12 mM sodium borate, pH 8.5 at 20°C.